journal

J. Am. Ceram. Soc., 79 [6] 1617–26 (1996)

Sources of Strain-Measurement Error in Flag-Based Extensometry

William E. Luecke* and Jonathan D. French*,*

Materials Science and Engineering Laboratory, National Institute of Standards and Technology, Gaithersburg, Maryland 20899

This paper examines the sources of error in strain measurement using flag-based extensometry that uses either scanning laser or electrooptical extensometers. These errors fall into two groups: errors in measuring the true gauge length of the specimen, which arise from the method of attachment of the flags, and errors arising from unanticipated distortions of the specimen during testing. The sources of errors of the first type include gauge-length errors from nonparallel flags and uncertainties in the true attachment point of the flag. During the test, strain-measurement errors of the second type can arise from horizontal translation of nonparallel flags, flag rotation that is induced by slippage, and flag motion from bending of the gauge length. Proper care can minimize the effect of these potential errors, so that flag-based extensometry can give accurate strain measurement, if appropriate precautions are taken. Measurements on silicon nitride indicate that the strain measurements are accurate to better than 10%.

I. Introduction

In the last 10 years, tensile creep and rupture testing of high-temperature ceramics have become increasingly common. Although contact extensometry has been used to measure creep of ceramics, the necessity of maintaining good contact between the specimen and the extensometer requires a lateral force on the specimen. This force, in turn, necessitates the use of a very stiff, self-aligning, and, hence, costly load train. Typically, the specimen then must project outside the hot zone of the compact furnace such that water-cooled grips can apply the load. Although this type of system yields excellent creep data, the requirement that the large specimen project outside the furnace precludes the testing of small specimens, such as those that may be produced from experimental grades of material. To test small specimens that are contained completely within the hot zone of the furnace, many laboratories have implemented flag-based, noncontact extensometry that uses either a scanning laser or electrooptical system. This paper investigates the potential errors in strain measurement using these noncontact methods. Gyekenyesi and Bartolotta[1] have produced an excellent review of a number of other types of extensometry for high-temperature tensile testing of ceramics.

Figure 1 shows the essential components of the system used by the authors in their laboratory. Most of the other laboratories that use similar systems have similar configurations. A light source illuminates the specimen through a slit cut in the furnace wall. In the scanning laser system,[1–16] a narrow (1–2 mm wide) laser is scanned vertically adjacent to the specimen gauge length. Two (or more) flags, either clipped[2–8,11,12,17] or glued[1,9,10,16] onto or integrated[13,18–22] into the specimen, project away from the gauge length and interrupt the light. The light (and the shadow of the flags) exits the furnace through a second slit and is projected onto a photodetector that is positioned behind the specimen. The time output of the detector is synchronized to the sweep of the laser; therefore, from the shape of the voltage–time output, it is possible to calculate the distance between the edges of the flags. It is important to realize that it is the shadow of the flag, rather than the flag itself, that defines the gauge length. There are several U.S. manufacturers of such systems, and the recently adopted ASTM standard for tensile creep of advanced ceramics[23] includes a section on scanning laser extensometry.

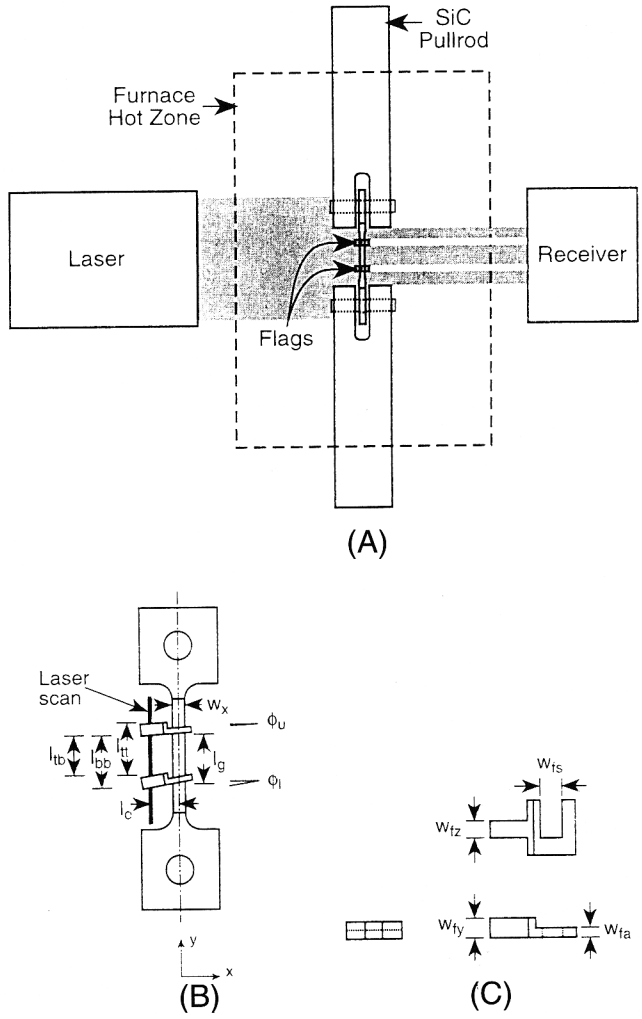

Fig. 1. Typical scanning laser extensometry system. Sketches of (B) NIST specimen and (C) gauge-length defining flags (see Table I for definition of terms).

P. F. Becher—contributing editor

Manuscript No. 192500. Received June 29, 1995; approved January 15, 1996.
Sponsored by the Ceramic Technology Project, DOE Office of Transportation Technologies, under Contract No. DE-AC05-84OR21400 with Martin Marietta Energy Systems, Inc.

*Member, American Ceramic Society.
*Guest Scientist, on leave from the Department of Materials Science and Engineering, Lehigh University, Bethlehem, PA 18015; now at Advanced Cerametrics, Lambertville, NJ 08530.

Instead of a scanning laser, the electrooptical extensometer[18,19,21,22,24,25] illuminates each flag with a high-intensity light source. Two flags still define the gauge length, but the system images the transition between the light flag and the dark background on a photocathode, which converts the optical image to an electron image that is, in turn, falls on an aperture that is positioned in front of a photomultiplier tube. Between the photocathode and the aperture is an electromagnet that deflects the electron image of the flag to maintain its position in the center of the aperture. The current necessary to keep the image of the flag in the center of the aperture is related to the distance that the flag has moved. However, similar to that which occurs in the scanning laser system, it is the edge of the flag that defines the gauge length.

Although the scanning laser and electrooptical methods are the most-common flag-based extensometry methods that are used for ceramics, there are several other similar methods of extensometry that use flags.[26–29] Some portions of the analysis in this paper may be applicable to these methods as well. In the diffraction system,[27] the two flags, either glued[28] or clipped[29] onto the specimen, form a narrow, horizontal diffraction slit, which a laser illuminates. As the specimen elongates, the slit widens, leading to a change in the interference pattern that is produced by the diffraction. From the spacing of the interference maxima, the slit width and, hence, the specimen elongation may be calculated.

The purpose of this paper is to address and quantify the potential strain-measurement errors in flag-based extensometry. For this reason, calculations are made by the authors, based on the geometry that has been used in their laboratory, to highlight how the analysis can be applied to the other systems and geometries when necessary. Errors that arise from the measurement units themselves are not considered. Under proper operation, the commercial measurement units typically guarantee a measurement repeatability of ~1 μm and linearity (i.e., maximum deviation from the "true" length reading) of several micrometers. The possible errors in strain measurement that are considered dwarf these absolute measurement errors.

II. Strain-Measurement Errors

Two types of errors may arise during strain measurement: gauge-length errors and deformation-induced errors. Gauge-length errors result from discrepancies between the true and measured gauge lengths of the specimen and can originate from nonparallel flags, a laser scan that is not parallel to the specimen, and the manner in which the flags are attached to the specimen. Deformation-induced errors originate from undesired deformations of the specimen during the test. Possibilities here include lateral movement of the specimen, bending of the specimen gauge length, droop of the flags caused by narrowing of the gauge section, and rotation of the flags about their long axis.

(1) Gauge-Length Errors

The first class of strain measurement errors originates from uncertainties in the gauge length, which are caused by the nature of the measurement itself rather than from deformations of the specimen. In the following discussion, repeated references to Figs. 1(B) and (C), which show the geometry of the flag attachment as implemented in this experiment, and Table I, which summarizes and defines the symbols that are used in the analysis, are made. The two flags, illustrated in Fig. 1(C), hang from the specimen at angles ϕ_u and ϕ_l. The flags interrupt the scanning laser beam a distance l_0 from the specimen centerline and define two gauge lengths, l_{tt} and l_{bb}, which are the distances between flag–laser scan intersections, as measured across the tops and the bottoms of the flags, respectively. These two lengths are the ones that are usually available in the commercial measurement systems. The true gauge length, which is discussed again later, is denoted by l_g; in this analysis, l_g is generally set to 10 mm. In a perfect experiment, $l_g = l_{tt} = l_{bb}$.

Table I. Symbols Used in This Analysis, with Typical Values*

Symbol	Typical value	Definition
l_g	10 mm	Gage length of specimen
l_0	5 mm	Offset of laser from specimen centerline
l_{tt}		Apparent gage length measured across the tops of the two flags
l_{bb}		Apparent gage length measured across the bottoms of the two flags
w_x	2.5 mm	In-plane sample width
w_z	2 mm	Out-of-plane sample width
w_{fy}	2 mm	Flag width, as seen by laser
w_{fz}	2 mm	Depth of flag perpendicular to scan
w_{fs}	2.6 mm	Flag attachment slot width
w_{fa}	1 mm	Width of flag at attachment point
ρ		Specimen bending radius
ϕ_u	5°	Upper flag attachment angle
ϕ_l	5°	Lower flag attachment angle
Ψ_u	0°	Upper flag rotation angle
Ψ_l	0°	Lower flag rotation angle

*Typical values used at the National Institute for Standards and Technology (NIST).

Although the figure shows the x-axis of the flag in the same plane as the head of the specimen, the flags often are mounted by the authors 90° to this orientation, such that the x-axis of the flag projects out of the page in Fig. 1(B).

When the flags hang at different angles from the specimen ($\phi_u \neq \phi_l$), the distance between them (l_{tt} or l_{bb}) does not reflect the true gauge length of the specimen accurately. Even slight deviations from absolute parallelism may introduce nonnegligible errors into the gauge-length measurement. Figure 2 shows the apparent gauge length that is produced for typical values of ϕ_l, the angle the lower flag makes with the specimen, while holding ϕ_u constant at 5°. For a typical specimen width, w_x = 2.5 mm, the flag attachment angle, ϕ, increases from 0° to 5° as the slot width of the flag clip, w_{fs}, increases from 2.5 to 2.6 mm. The gauge-length error that is caused by nonparallel flags can approach 5% (500 μm in a gauge length of 10 mm) for very small differences in the flag attachment angles. Some laboratories produce flags in which the slot is cut at a slight angle to the y-axis of the flags, producing a flag that can hang with an attachment angle of 0°. Although this method does remove the sidewalls of the flag slot from the surface of the specimen, which may be important if the specimen oxidizes severely during the test, it also increases the cost of the flag. The measurement error that is introduced by nonparallel flags still is controlled completely by the tolerance on w_{fs}, a problem that the use of an angled-slot flag does not address.

A potentially more-serious problem is the uncertainty in the actual flag attachment point itself. At elevated temperature,

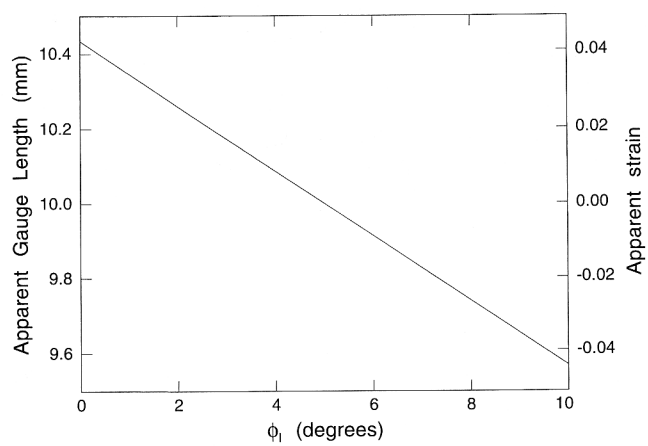

Fig. 2. Effect of nonparallel flags on measured gauge length. Here, true gauge length, l_g, is set to 10 mm (upper flag attachment angle, ϕ_u, is 5°; l_0 is beam offset, 5 mm).

friction, which is usually aided by the oxide that forms on both the flag and specimen surfaces, holds each flag to the specimen at two points (see Fig. 1(B)); both of these points lie within the creeping section of the specimen. To a first approximation, neglecting dimensional change of the specimen during creep, these two points on the flag cannot remain rigidly attached to the specimen surface during creep, because creep is increasing the distance between them. As a result, only one of the points on the flag may remain rigidly attached to the specimen; the other must slide. The length of specimen that is producing the increasing separation of the flags may be as much as $l_g + w_{fa}$ or as little as $l_g - w_{fa}$, assuming parallel flags are attached with $\phi_l = \phi_u = 0°$. The former case corresponds to that where the outermost points remain attached during creep, whereas the latter corresponds to the case where the inner points remain attached to the specimen. For reasonable choices of the l_g and w_{fa} values (10 mm and 1 mm, respectively), this uncertainty is $\pm 10\%$ of the true gauge length.

The use of glued-on or integral flags does not solve this problem, however. Glued-on flags are attached over their entire length, at least at room temperature at the start of the experiment. During creep, the glue, typically a high-temperature adhesive, must deform or crack as the material beneath the glue joint creeps, which produces the same sort of attachment point uncertainty that is seen for the clipped-on flags. From a test-to-test repeatability standpoint, glued-on flags may be slightly inferior to the clipped-on type, because there is no way to ensure that the glue will crack in the same manner during each test. With clipped-on flags, the attachment point is likely to be the same from test to test, although it may not be easily characterized. In the integral-flag design, the flag is actually a part of the specimen that projects out from the gauge length and is usually about the same size as the clipped-on flags in Fig. 1(C). There is a transition from the uniform cross-sectional-area gauge length to the flag; therefore, the distance between the flags (l_{tb} in Fig. 1(B)) is not of uniform cross section. If the gauge length is taken as the interior distance between the flags (l_{tb} in Fig. 1(B)), the creep will not be uniform in the measured gauge length, which results in a strain-measurement error. Alternatively, if the gauge length is taken as the length that is of constant cross section, there will be creep outside this length in the transition region to the flag, which leads to an overestimate of the creep strain. Of course, it may be possible to correct for the nonuniformity of creep in the measured gauge length, but, generally, the creep properties of the material are unknown, which makes such a correction difficult. Integral flags, however, may offer slightly improved test-to-test repeatability over the clipped-on flags, because it should be easier to machine the specimens to the exacting tolerances than to guarantee the repeatable attachment of the clipped-on flag.

There are two strategies to combat the attachment-point uncertainty. The first is to make the gauge length as long as possible, to minimize the contribution of the attachment-point uncertainty. A second approach is to make the width of the flag as narrow as possible (w_{fa} in Fig. 1(C)), which is what the authors have done with their flag. Of course, narrowing the attachment width also weakens the flag. Because the flags sometimes break when the specimen fails, the design of the authors is a compromise between measurement accuracy and flag survivability.

In measurement systems where the flag is clipped or glued onto the specimen, it is inappropriate to use the inside distance between the flags (denoted by l_{tb} in Fig. 1(B)) as a measure of the gauge length. Because the flags are nominally identical, they have a tendency to attach at the same point; therefore, the gauge length should be measured between two identical points on the flags. A more correct measure of the gauge length, then, is the distance between either the tops or the bottoms of the flags. Of course, in the integral-flag geometry, l_{tb} is the more appropriate measure.

(2) Errors Originating from Deformations

The second class of errors originates from undesired deformations of the specimen and unanticipated motions of the flags. These deformations include horizontal translation of nonparallel flags, flag droop during creep, flag rotation, and bending of the gauge length.

(A) Horizontal Translation of Nonparallel Flags: When the flags are not parallel, strain-measurement error can occur if the loading train shifts laterally, relative to the laser scan, such as that which may occur when temperature changes in the room distort the loading frame. The net effect is that the laser intercepts a different part of each flag, which produces spurious changes in specimen length. Measurements of the widths of actual specimens and attachment slots of the flags (w_{fs}) indicate that the flags may hang at angles of 0°–10°. Figure 3 shows that the gauge length may appear to change by up to 10 μm for lateral shifts of only 200 μm when the flags differ in attachment angle by as little as 3°. Considering that the typical extension to failure for creep-resistant silicon nitride is only ~100 μm for a gauge length of 10 mm, this apparent length change may introduce strain-measurement errors of ~10%.

(B) Flag Droop during Creep: When the specimen strain becomes large during constant volume deformation, such as in superplastic deformation, the specimen width must decrease, which causes the flag to droop. Precisely parallel flags droop at

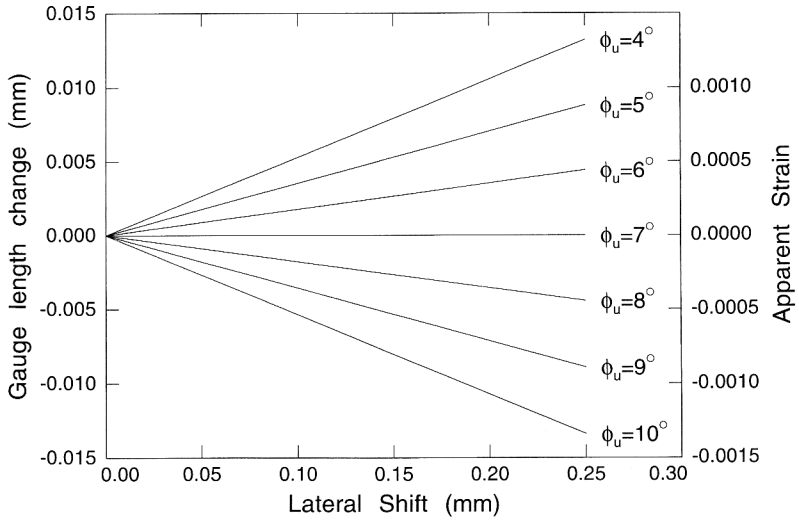

Fig. 3. Changes in apparent strain and gauge length when loading train shifts, relative to laser, for different upper flag attachment angles, ϕ_u (lower flag attachment angle, ϕ_l, is 7°).

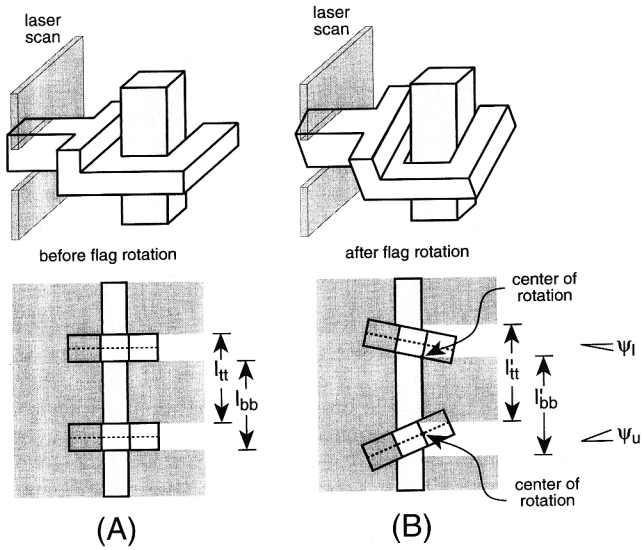

Fig. 4. Flag rotation can alter apparent gauge length of specimen. (A) View down x-axis of flags before rotation; flags have same geometry as those in Fig. 1(B). (B) View down x-axis of flags after rotation (ideally, $\Psi_u = \Psi_l = 0$).

the same rate, so the l_{tt} and l_{bb} gauge lengths remain constant. If the flags begin the experiment nonparallel ($\phi_l \neq \phi_u$), l_{tt} and l_{bb} will not remain equal during the experiment. Fortunately, for flags that are nearly perpendicular to the specimen ($0° \leq \phi \leq 10°$), the changes in l_{tt} and l_{bb} are nearly linear with the change in attachment angle; therefore, almost no additional error beyond the mismeasurement of the original gauge length (Section II(*1*)) occurs as the flags droop.

(C) Flag Rotation: Dramatic gauge-length measurement errors occur when one or both flags rotate about their long axes (the x-axis in Fig. 1(B)) during the test. Because friction holds the flags onto the specimen, such rotation may occur if a flag is unbalanced, which leads to moments about the x-axis. Frequently, the authors have observed such rotation during heating, when the cellulose glue that holds the flags in place at room temperature burns away. The sliding that must occur at the attachment points of the flags (see Section II(*1*)) also may result in the rotation of the flag. Figure 4, which shows the flags in a view down the x-axis, illustrates rotation about the x-axis of the flag (also see Fig. 1(C)). In the figure, the shaded region represents the scan of the laser beam, and the unshaded regions correspond to the dark areas where the flags have blocked the beam; the laser is to the left, and the receiver is to the right. It seems unlikely that the flag, if it rotates, will do so around the center of its arm. Rather, it seems more probable that the rotation will occur about one of the two lines that form the bottom of the slot that clips the flag onto the specimen. Then, in Fig. 4, the top flag, which is rotating clockwise, does so about a point on the bottom edge of the flag. In contrast, the bottom flag, which is rotating counterclockwise, does so about the top attachment point, which is *not* at the highest point on the flag.

During flag rotation, the position of the upper and lower corners of the flags, which define l_{tt} and l_{bb}, will follow the equation of a circle whose radius is the distance from the relevant corner to the center of rotation. For a clockwise rotation (see the top flag in Fig. 4), the upper corner of the flag moves up, while the lower corner may move either up or down, depending on the depth of the flag, w_{fz}. Figure 5 shows that, as the flag becomes wider, the measurement error increases. In this simulation, one flag rotates (in this case, the top flag turns clockwise) while the other remains fixed. This simulation is only one of a huge number of possible combinations and simply illustrates the magnitude of the possible error. Because of the asymmetry of the attachment point of the flag, l_{tt} and l_{bb} provide different values for the apparent gauge length. The example shows a positive apparent strain for l_{tt} but, for some cases, an apparent negative strain for l_{bb}. Similar to that which is

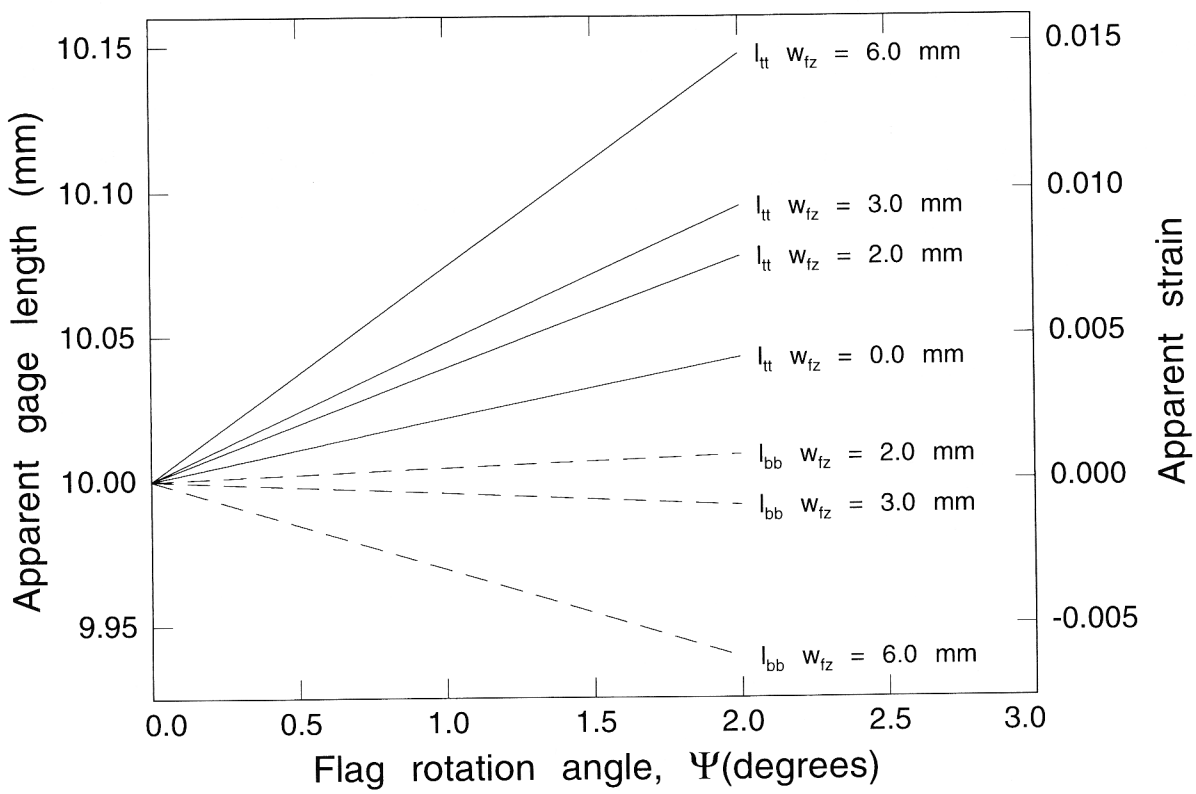

Fig. 5. Effect of one possible flag rotation of apparent gauge length for true gauge length of 10 mm calculated for various flag depths (w_{fz}). Upper flag rotates clockwise (see Fig. 4) while lower flag remains rigidly attached. Because upper flag rotates about edge of specimen rather than its center, l_{tt} increases monotonically while l_{bb} first increases then decreases as w_{fz} increases.

observed with the lateral shift of the laser scan during the test (Section II(2)(*A*)), although absolute length changes are small, they can be on the order of the total extension that is measured during a creep test.

Because the measurement error increases with increasing w_{fz} (Fig. 5), the authors have reduced the depth of the flag to 2 mm. This thickness represents a compromise between a desire for increased accuracy and increased durability of the flags. Although it may seem that using a round flag arm will remove the error that is caused by flag rotation, this is not the case. During any rotation of a round flag (except the unlikely case of rotation about the center of the circular arm itself), l_{tt} and l_{bb} change but remain equal to each other; therefore, the rotation still will produce an apparent strain. During a test using flags with rectangular cross sections, it is possible to detect flag rotation, but not to correct for it, by monitoring the apparent width of the individual flags. If the flags have a round cross section, their apparent width does not change when the entire flag rotates. In Fig. 5, the calculation for $w_{fz} = 0$ (the zero-depth flag) very closely approximates the strain-measurement error from round flags of any radius. Thus, although the absolute error for equal rotations is about half as large for round flags as it is for rectangular flags, it also is, unfortunately, undetectable. In addition, it is much more expensive to fabricate the round flags. The calculation for the zero-depth flag is applicable to a flag whose arm has a diamond cross section. Because the edges of the flag that the extensometer images are closer together, the rotation error is less than for a flag with an equally sized square cross section. However, as with the round flags, the fabrication costs are higher.

In all of this discussion of flag rotation and specimen bending, it is important to keep in mind that it is generally not easy to correct for these errors. Although the discussion assumes that the flag edge defines the gauge length, both the electrooptical and scanning laser extensometers image the shadow of the three-dimensional flag rather than the flag edge itself. It is not possible, from the image of the flag alone, to know what type of deformation has caused an apparent change in width.

(D) Bending of Gauge Length: There have been many reviews of the effects of bending on lifetime and strain to failure (ε_f) of tension specimens, for example, those of Christ and Swanson[30] and Hayhurst.[31] These studies focused on the effects that the bending stresses may have on the deformation of the material. The focus in this paper is to examine the magnitude of the error that bending of the gauge length produces on the apparent strain. Bending of the specimen during loading can occur when the loading line does not lie on the centerline of the gauge length, which may happen when the loading holes are off-center, with respect to the gauge centerline. During bending of the gauge length, the positions of the flags may shift, producing apparent extensions, which do not reflect the true specimen extension due to creep.

Two types of bending of the gauge length that may introduce strain-measurement errors have been identified by the authors. The first, which is termed "arc bending," has been analyzed by Christ and Swanson.[30] When the loading line does not lie along the gauge centerline, the load applies a small bending moment to the gauge section, in addition to the uniaxial load. The simplest case to consider is one where the loading line is uniformly displaced to one side of the gauge centerline. In an elastic analysis, the displacement will produce a moment that will tend to bend the specimen to an arc of a circle (Fig. 6(B)). For instance, for the specimen shown in Fig. 1, if the loading line is displaced 25 μm from the gauge centerline, the resulting moment will produce a 9% increase in the surface stress on one of the faces over the applied uniaxial stress, as well as a bending of the specimen to a radius of curvature of 50 m. A more-complex bending may occur when the loading line crosses the gauge centerline. In this case, the specimen will bend elastically to an "S" shape (Fig. 6(C)); this discussion will not address this deformation mode. A second type of bending has become evident during examination of crept specimens to assess the curvature of the gauge length that arc bending may produce. This type of bending is called "hinge bending," because all the deformation of the specimen is concentrated near the ends of the gauge length, rather than being distributed evenly through the gauge length, as in arc bending. Figures 6(D) and (E) illustrate hinge bending where the loading line is displaced

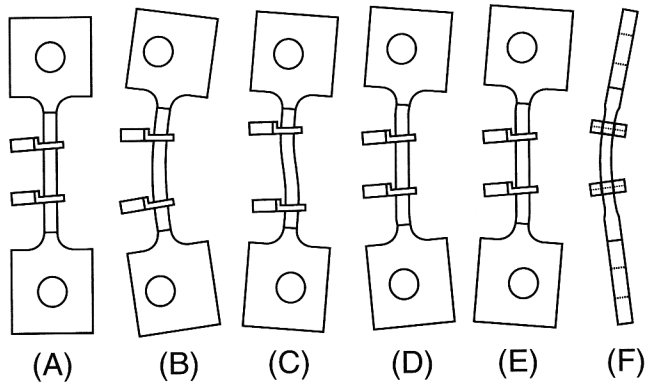

Fig. 6. Various types of specimen bending associated with misalignment of loading axis, with respect to specimen gauge centerline: (A) undeformed specimen; (B) arc bending; loading points are displaced to same side; (C) arc bending; loading points are displaced to opposite sides; (D) hinge bending; loading points are displaced to same side; (E) hinge bending; loading points are displaced to opposite sides; and (F) out-of-plane bending. (Distortions are grossly exaggerated.)

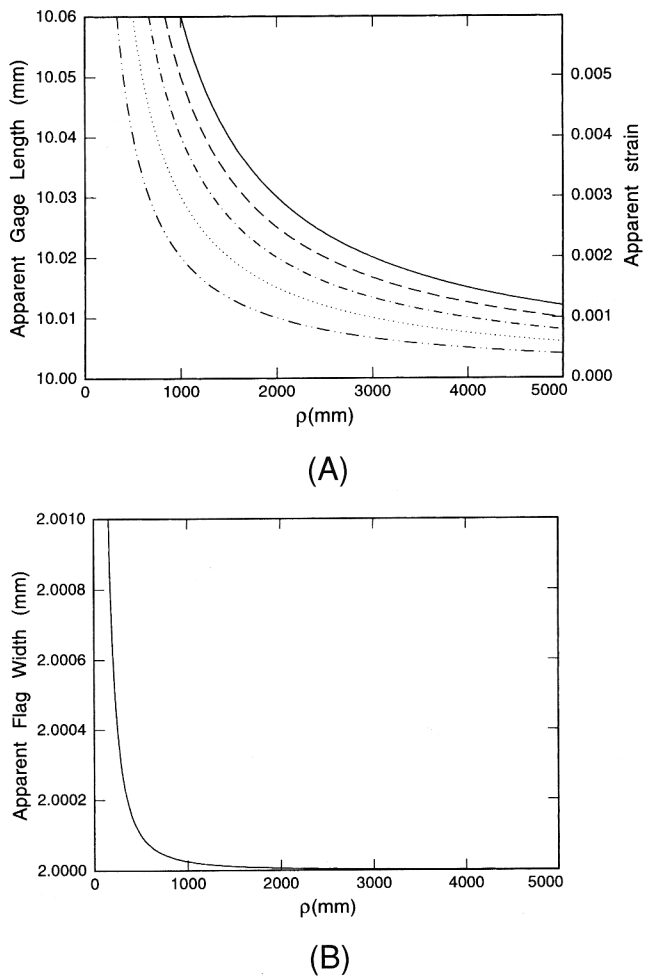

Fig. 7. Effects of in-plane bending on apparent gauge length: (A) apparent gauge length, for different beam offsets (l_0 values of (—) −6, (– –) −5, (– · –) −4, (····) −3, and (– · · –) −2 mm), based on true gauge length of 10 mm, and (B) apparent flag width, for $\phi = 0°$, as functions of bending radius (ρ).

away from the gauge length and where it crosses the gauge length, respectively.

(a) Arc Bending of Gauge Length: To simplify the calculation of the flag positions during arc bending, the authors assume that the specimen bends to a constant radius of curvature, as may happen if a pure bending moment is applied to the gauge length. The calculations that follow do not include any specimen extension; rather, they demonstrate the apparent extension that bending of the gauge length produces.

For the case in which the specimen deforms by bending in the plane of the specimen head (termed "in-plane bending"), the motion of the flags will tend to magnify the effect of the bending. In the geometry that has been considered in this paper, the distance from the geometric center of the specimen to the laser scan remains constant, although, in reality, the bending may cause the specimen to shift as well. In that case, there will be lateral translation errors (Fig. 3) as well. The bending may cause the apparent gauge length to increase or decrease as the laser intercepts a different part of each flag, depending on whether the flags are diverging or approaching.

Figure 7(A) shows the apparent gauge length of the specimen as a function of the radius of curvature (assuming a true gauge length of 10 mm, typical for the experiments of the authors) for the case where the specimen bends away from the laser scan, which results in increases in apparent gauge length. To put the radius of curvature into proper perspective, when the 2 mm × 2.5 mm specimen bends to a radius of curvature of 1000 mm, the neutral axis translates 10 μm in the x-direction from its original position. As with most of the other simulations in this paper, no axial strain has been added to the specimen. The apparent strains simply are those that will be measured if the specimen bends without creeping. Figure 7(A) shows that the strain mismeasurement that is caused by bending increases as the beam offset, l_0, increases. For the specimen geometry of Fig. 1, when $l_0 = -1.25$ mm, the laser scan lies against the edge of the specimen. If the specimen is grossly distorted (i.e., bent to a small radius of curvature), the strain-measurement error can become quite large, perhaps as large as the expected strain during a creep test of silicon nitride. To minimize these errors, the laser scan is positioned as closely as possible to the edge of the specimen.

Figure 7(B) shows that, although the bending may induce a large strain-measurement error, it will be undetectable by monitoring the apparent widths of the flags. However, increasing the attachment angle of the flag does not substantially increase the strain-measurement error for small attachment angles; thus, precisely perpendicular flags ($\phi = 0°$) are not necessary for measurement accuracy.

The specimen also may experience "out-of-plane" bending, seen in Fig. 6(F), in which the specimen deforms by bending out of the plane that is defined by the specimen head. This type of bending may arise if the loading-pin pressure bears preferentially on the outside edge of the loading hole rather than evenly through its depth. To combat this off-axis loading, the edges of the loading hole are generally chamfered to ~1/3 the depth of the specimen head. As the specimen bends toward the laser, for example, the back edge of the top flag and the front edge of the bottom flag move up and forward. The l_{tt}-defined gauge length changes, and the apparent width of the flag increases. Unlike the case of in-plane bending, the depth of the flag (w_{fz}) and the position of the flags along the gauge length influence the gauge-length-measurement error. Figure 8(A) shows the apparent gauge length, again assuming the default values shown in Table I, as a function of bending radius (ρ). When the flags are attached symmetrically about the centroid of the specimen (gauge-length center = 0.0 in Fig. 8(A)), their motion nearly cancels; therefore, out-of-plane bending produces no apparent strain. If the center of the flag-defined gauge length is not on the centroid of the specimen, however, the motion no longer cancels, because one flag moves farther toward the laser than the other, and the apparent length change is much larger. The family of curves in Fig. 8(A) shows the

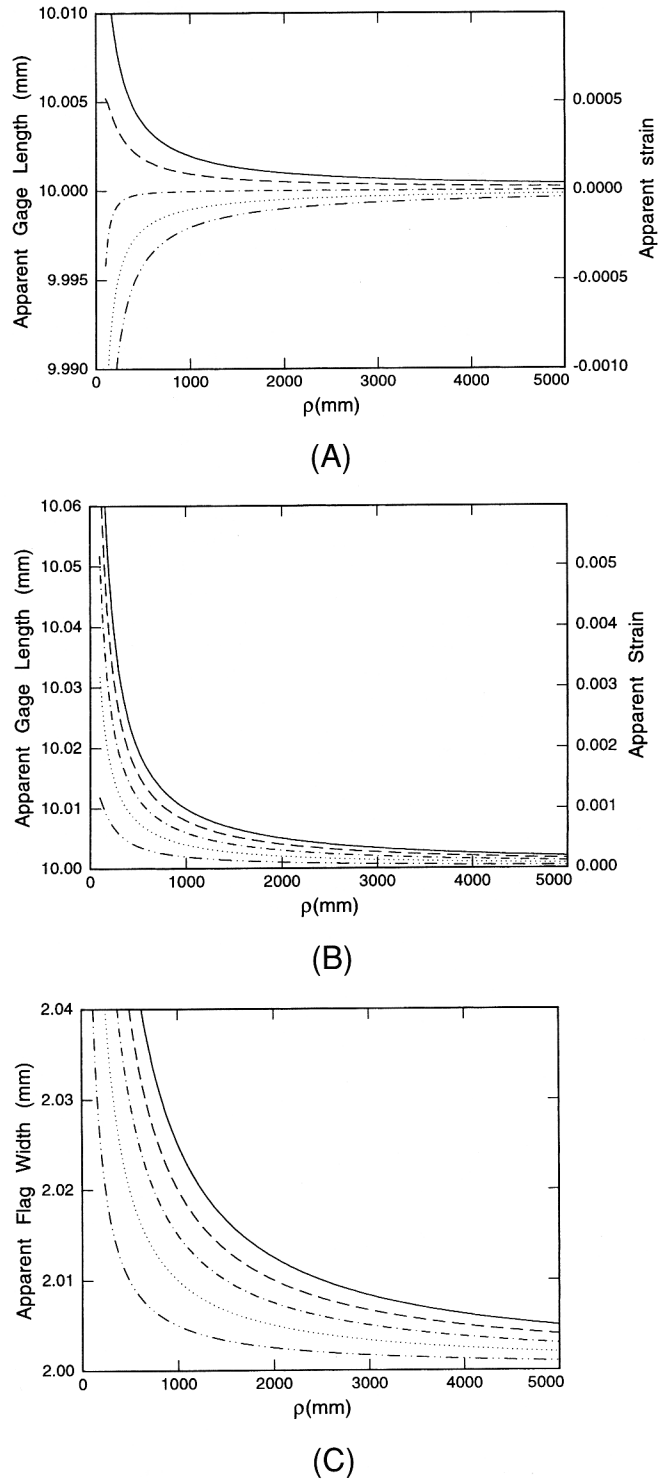

Fig. 8. Effects of out-of-plane bending on apparent gauge length: apparent gauge length as function of ρ for (A) gauge length of 10 mm, with flags attached at different points along gauge length (w_{fz} = 2 mm; gauge-length centers of (—) 1.0, (– –) 0.5, (– · –) 0.0, (· · · ·) −0.5, and (– · · –) −1.0 mm), and (B) various w_{fz} ((—) 5, (– –) 4, (– · –) 3, (· · · ·) 2, and (– · · –) 1 mm; center of flag-defined gauge length is 2 mm above geometric center of specimen). (C) Apparent flag widths, given in Fig. 8(B), as function of ρ (w_{fz} values of (—) 5, (– –) 4, (– · –) 3, (· · · ·) 2, and (– · · –) 1 mm).

change in apparent gauge length during bending when the center of the flag-defined gauge length lies above, on, and below the geometric center of the specimen.

The mismeasurement of the gauge length is not as severe for out-of-plane bending as it is for in-plane bending, and the gauge

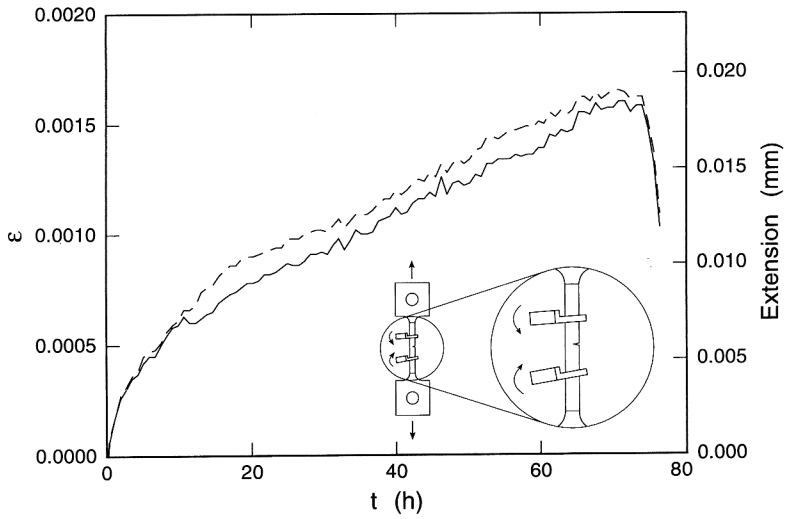

Fig. 9. Apparent negative tertiary creep (which occurs when opening of creep crack (see inset) causes in-plane sample bending), which leads to motion of flags. For two flags, strains that are measured across (—) tops (ε_{tt}) and (– –) bottoms (ε_{bb}) are in reasonable agreement, and increase in apparent widths is extremely small during test.

length can appear to contract as well. Figure 8(B) shows the apparent gauge length for different w_{fz} when the center of the flag-defined gauge length is offset 2 mm from the geometric center of the specimen. Finally, Fig. 8(C), which relates the apparent flag widths for Fig. 8 to ρ, shows that the apparent width of the flag also increases as w_{fz} increases when the flags are displaced from the geometric center of the specimen. Unlike the in-plane bending case, the strain-measurement error is not large, in contrast to the large change that is possible in apparent flag width.

The change in apparent flag width is large for rather insignificant strain-measurement errors during out-of-plane bending, which dilutes the effectiveness of the apparent flag width as a diagnostic tool for bending detection. The appearance of changes in apparent flag width during the test can signal flag droop (Section II(2)(*B*)), flag rotation (Section II(2)(*C*)), or out-of-plane arc bending. Of these three, flag rotation produces the greatest error; the other two are fairly innocuous. In contrast, in-plane bending, which may produce significant strain-measurement errors, produces little to no change in apparent flag width. To confound matters, it is impossible to know which effect is producing the change in apparent flag width if only the apparent flag width is known. Therefore, the appearance of a change in the apparent flag width during a test may indicate that a test is giving strain-measurement error, but a constant apparent flag width during a test does not guarantee that no strain-measurement error has occurred.

The opening of a crack in the gauge length between the flags can produce the appearance of tertiary creep, which is actually caused by the same motion of the flags that arc bending produces. Figure 9 shows the creep curves from a specimen of reaction-bonded silicon carbide (SCRB210, Coors Porcelain Co., Golden, CO), which was tested at 1375°C and 110 MPa, that shows apparent "negative" tertiary creep. During the test, the apparent widths of the upper and lower flags varied by <1 μm. Examination of the specimen after failure showed that a crack grew from the corner of the specimen on the opposite side of the flags (see inset, Fig. 9). Evidently, the opening of this crack produced a rotation of the flags similar to that which is produced by in-plane arc bending. Because the change in apparent flag width is not a sensitive indicator of in-plane bending, there was no way—other than the obvious improbability of negative tertiary creep—to infer that this experiment was not yielding correct data. If the crack had grown from the other side, the tertiary creep would appear positive rather than negative and, therefore, completely reasonable, although an artifact in the strain-measurement process produced it.

(b) Hinge Bending of Gauge Length: Figure 10 shows the measured centerline of a specimen of crept silicon nitride[32] (PY6, vintage 1991, GTE Corp., Waltham, MA) that exhibited hinge bending. The origin of the coordinate system was defined as the intersection of a line connecting the centers of the two loading holes and its perpendicular bisector. In a "perfect" specimen, this point also is the centroid of the specimen. The curvature of the gauge length amounted to <5 μm of displacement of the centerline from linearity and corresponded to a radius of curvature of >10 m. It is clear from the measurements that the specimen heads are grossly bent away from the gauge centerline, such that the distortion is even visible to the naked eye. Creep must have caused the distortion, because the centerlines of the heads began the test parallel. During the test, the specimen exhibited no warning of this bending. The apparent flag widths remained constant to within 5 μm, and the l_{tt} and l_{bb} strains agreed to within 5%.

Although the authors do not understand the reason for the localization of the deformation at the end of the gauge length during hinge bending, it probably originates when the load is applied off the axis of the specimen gauge length, by either poorly aligned loading holes or loading pins that are held off-center by frictional forces. There are two generic ways that the specimen can be loaded off-axis—symmetrically and antisymmetrically. In the symmetric case, the loading points are shifted to the same side of the gauge-length centerline; whereas, in the antisymmetric case, the holes are shifted to opposite sides. For the symmetric case, as the holes align with the gauge length, the gauge length translates in the *x*-direction (see Fig. 6(D)). This translation produces errors such as those that are described in Fig. 3. Even for extremely poorly manufactured specimens, with loading holes >50 μm from the gauge centerline, the change in apparent strain is <0.0005, corresponding to a change in the gauge length of only 5 μm. When the holes are displaced antisymmetrically, the effect is similarly small. Although this type of bending may seriously change the rupture lifetime of the specimen, its effect on the measured strain is minimal.

III. Flag-Based Extensometry in Practice

The previous sections have examined the possible errors that are associated with flag-based extensometry. In many places, "worst-case" scenarios deliberately have been assumed by the authors, a practice that may cause potential users to have misgivings about adopting the technique. To dispel these fears, the results of an investigation are presented briefly, in an attempt to

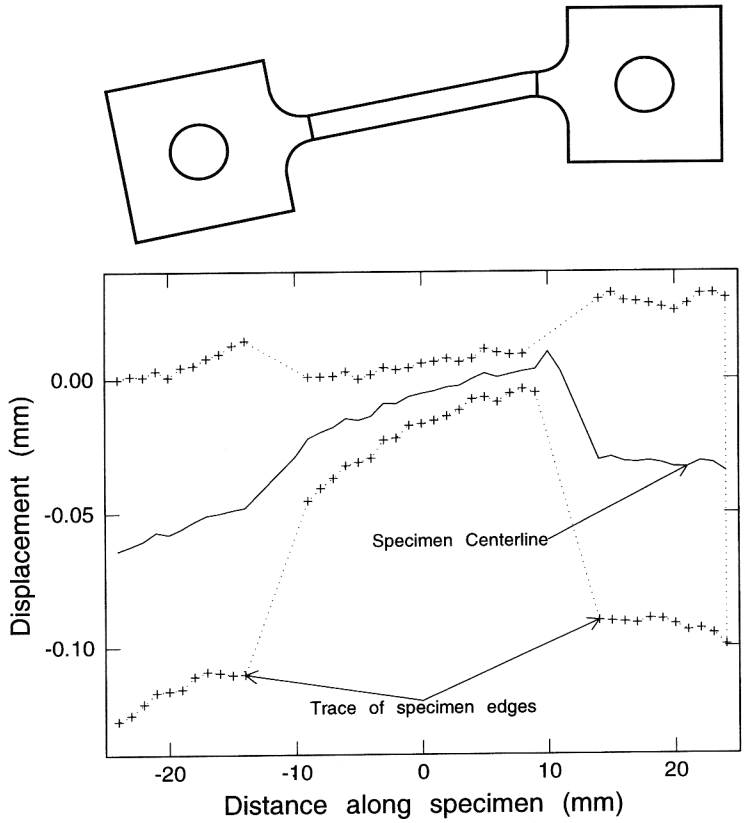

Fig. 10. Specimen centerline of silicon nitride specimen, crept to $\varepsilon = 0.0054$ at 104 MPa and 1350°C (trace of (—) centerline of specimen gauge length and (+) specimen edge suitably shifted in *y*-direction to lie on same axis as specimen centerline). Note that gauge length has remained relatively straight during creep, but bending deformation is concentrated near end of gauge length. Distortion of accompanying specimen diagram is exaggerated.

measure the strain in a number of specimens independently and correlate it with the strain that is measured by scanning laser extensometry.

A previous investigation[2] demonstrated that, over a fairly wide stress and temperature range, the volume fraction of cavities in the gauge length of a crept specimen increased linearly as strain increased. The authors observed that same behavior in a suite of replicated tests on another silicon nitride (GN10, AlliedSignal, Torrance, CA).[33] In this set of experiments, a number of specimens of two different geometries were crept to failure under the same conditions (1275°C, 137.5 MPa). Failure strains ranged from 0.0048 to 0.0105. Figure 11 shows that the linear correlation between ε_f and cavity volume fraction (f_v) that was observed previously[2] also occurred here; thus, it was possible to use f_v as a measure of the true strain and, thereby, assess the veracity of the measured ε_f.

With the exception of the uncertainty in attachment point of the flag (Section II(*1*)) and the concomitant uncertainty in the true gauge length, all of the other strain-measurement errors (nonparallel flags, horizontal translation during creep, flag rotation, and bending) are as likely to overestimate true strain as to underestimate it. Therefore, the best-fit line in Fig. 11 represents the average relationship between f_v and measured ε_f. The deviations from the best-fit line are, then, an estimate of the maximum error in the measured strain. Typically, that deviation is ~5%, and the maximum deviation is only 13%; thus, the error in the strain that is measured using laser extensometry is probably <10%.

IV. Application of These Calculations to Similar Methods

The preceding analysis has focused on experimental conditions germane to this experiment, although most other laboratories that use the scanning laser method use a very similar configuration. Some of the possible measurement errors also can affect strain measurements by the electrooptical extensometer and the diffraction method. In particular, the attachment point uncertainty (Section II(*1*)) plagues these two techniques as well. Nonparallel flags can introduce strain-measurement error to the results of the electrooptical exensometer, but because practitioners of this technique usually use integral flags, it probably is not a serious issue. Out-of-plane bending

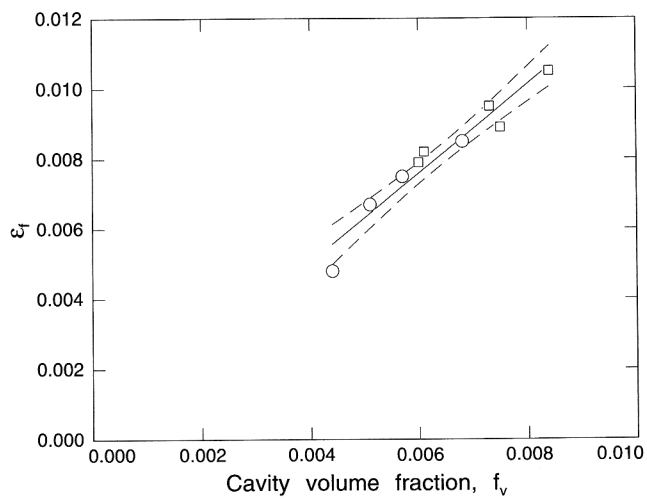

Fig. 11. Measured strain to failure (ε_f) as function of measured cavity volume fraction (f_v) for nine silicon nitride specimens ((□) 76 and (○) 50 mm) tested at 137.5 MPa and 1275°C. Linear correlation between ε_f and f_v that has been observed earlier holds true here as well. Dashed lines represent 90% confidence interval for fit.

Table II. Assessment of Severity of Various Strain-Measurement Errors

Error	Paper section	Severity of error
Flag rotation	II(2)(C)	Rotations of the flags by as little as 1° or 2° can create strain-measurement errors on the order of 100%
Attachment-point uncertainty	II(1)	Can be as large as 10% for short gauge lengths and wide flags, but probably does not change from test to test
Nonparallel flags	II(1)	Can be as large as 10% for specimens with small gauge length and large l_0
Horizontal translation of nonparallel flags	II(2)(A)	Difficult to quantify; can be up to 10% for very small horizontal translations of the load train
Arc bending of the gauge length	II(2)(D)	For bending to small radii of curvature, the strain-measurement error can be very large; has not been observed by the authors in silicon nitride
Flag droop	II(2)(B)	Insignificant for small strains
Hinge bending of the gauge length	II(2)(D)	Even for large specimen deformations, the strain-measurement error remains small

also affects both techniques. Because the electrooptical extensometer tracks the position of the edge of the flag, it will perceive the out-of-plane bending in the exact same manner that the scanning laser extensometer does—as apparent extension. In the diffraction technique, out-of-plane bending will tend to change the slit width, but in a manner that is specific to the method in which the slit is formed. The effect of in-plane bending on the electrooptical extensometer is identical to that of the laser extensometer. The width over which the extensometer images the transition from the dark background to the bright flag can be as small as several hundred micrometers, which is less than that for the laser extensometer. Rotation of the flag will produce the same apparent change in gauge length that rotation of the flag does in scanning laser extensometry.

One important limitation of the commercial electrooptical extensometers that have been examined is that they can track the position of, at most, two edges during the test. In contrast, the two commercial laser extensometers can track the positions of many edges nearly simultaneously. The electrooptical extensometer, then, can track neither the apparent flag widths nor the second gauge-length measurement, both of which are useful diagnostics of the quality of an experiment.

V. Summary and Specific Recommendations

Table II ranks the major potential sources of strain-measurement error in order of severity. Of the potential errors, unwanted flag rotation can be the most severe. Attachment-point uncertainty plagues all tests with all types of flags. The errors that are caused by nonparallel flags can be countered by careful manufacture of the flags. Arc bending has the potential to introduce significant errors, but it does not seem to occur in the materials that the authors have tested. The bending that does occur in misaligned specimens (hinge bending) produces little strain-measurement error. Flag droop during creep probably results in insignificant errors.

Although scanning laser extensometry can give accurate measurements of strain, this paper has some specific recommendations to minimize the possible error that is involved:

(1) To minimize the attachment-point uncertainty, the clip of the flag should be as narrow as possible. This caveat applies to glued-on flags as well.

(2) The flags should hang at the same angle, to allow their separation to reflect the true gauge length, as well as to minimize errors that are induced by shift of the loading train or laser scan.

(3) The flags should be balanced to avoid moments that might lead to flag rotation, because flag-rotation errors are some of the largest potential errors.

(4) The alignment of the loading holes, with respect to the gauge-length centerline, must be of the highest accuracy to eliminate the bending moments that lead to specimen deformation. Although the hinge bending in this paper that has been observed in silicon nitride is relatively harmless, as far as strain-measurement error is concerned, arc bending of the gauge length may occur in other materials.

(5) For a test to be considered successful, the strain that is measured across the tops and bottoms of the flags (ε_{tt} and ε_{bb}, respectively) should agree. The appearance of apparent flag-width change during the test may indicate that strain-measurement error is occurring.

References

[1]J. Z. Gyekenyesi and P. A. Bartolotta, "An Evaluation of Strain Measuring Devices for Ceramic Composites," *J. Test. Eval.*, **20**, 285–95 (1992).

[2]W. E. Luecke, S. M. Wiederhorn, B. J. Hockey, R. F. Krause Jr., and G. G. Long, "Cavitation Contributes Substantially to Tensile Creep in Silicon Nitride," *J. Am. Ceram. Soc.*, **78** [8] 2085–96 (1995).

[3]S. M. Wiederhorn, B. J. Hockey, D. C. Cranmer, and R. Yeckley, "Transient Creep Behavior of Hot Isostatically Pressed Silicon Nitride," *J. Mater. Sci.*, **28**, 4445–53 (1993).

[4]B. J. Hockey, S. M. Wiederhorn, W. Liu, J. G. Baldoni, and S.-T. Buljan, "Tensile Creep of Whisker-Reinforced Silicon Nitride," *J. Mater. Sci.*, **26**, 3931–39 (1991).

[5]H.-T. Lin, P. F. Becher, and M. K. Ferber, "Improvement of Tensile Creep Displacement Measurements," *J. Am. Ceram. Soc.*, **77** [10] 2767–70 (1994).

[6]C. J. Gasdaska, "Tensile Creep in an *In Situ* Reinforced Silicon Nitride," *J. Am. Ceram. Soc.*, **77** [9] 2408–18 (1994).

[7]S. Haig, W. R. Cannon, and P. J. Whalen, "Anelastic Recovery in Crept Silicon Nitride," *Ceram. Eng. Sci. Proc.*, **13** [9–10] 1008–23 (1992).

[8]J. A. Wade, C. S. White, and F. J. Wu, "Predicting Creep Behavior of Silicon Nitride Components Using Finite Element Techniques"; pp. 360–72 in *Life Prediction Methodologies and Data for Ceramic Materials, ASTM STP 1201*. Edited by C. R. Brinkman and S. F. Duffy. American Society for Testing and Materials, Philadelphia, PA.

[9]J. Sankar, S. Krishnaraj, R. Vaidyanathan, and A. D. Kelkar, "Elevated Temperature Behavior of Sintered Silicon Nitride Under Pure Tension, Creep, and Fracture"; see Ref. 8, pp. 19–35.

[10]N. Dey and D. F. Socie, "Tensile Creep Behavior of Alumina under Static and Cyclic Loading," *Ceram. Eng. Sci. Proc.*, **15** [5] 634–41 (1994).

[11]J. D. French, J. Zhao, M. P. Harmer, H. M. Chan, and G. A. Miller, "Creep of Duplex Microstructures," *J. Am. Ceram. Soc.*, **77** [11] 2857–65 (1994).

[12]D. F. Carroll, S. M. Wiederhorn, and D. E. Roberts, "Technique for Tensile Creep Testing of Ceramics," *J. Am. Ceram. Soc.*, **72** [9] 1610–14 (1989).

[13]J. A. G. Furness and T. W. Clyne, "The Application of Scanning Laser Extensometry to Explore Thermal Cycling Creep of Metal Matrix Composites," *Mater. Sci. Eng. A*, **141**, 199–207 (1991).

[14]K. Hatanaka, H. Shiota, and T. Ando, "Tensile Test of Sintered Silicon Nitride Ceramic at Elevated Temperature," *JSME Int. J., Ser. 1*, **34** [3] 351–60 (1991).

[15]S. Luszcz, Lanxide Corp., Newark, DE; personal communication, 1995.

[16]R. Beigel, U.S. Naval Research Laboratory, Washington, DC; personal communication, 1995.

[17]D. C. Cranmer, B. J. Hockey, S. M. Wiederhorn, and R. Yeckley, "Creep and Creep Rupture of HIP'ed Si_3N_4," *Ceram. Eng. Sci. Proc.*, **12** [9–10] 1862–72 (1991).

[18]D. F. Carroll and R. E. Tressler, "Effect of Creep Damage on the Tensile Creep Behavior of a Siliconized Silicon Carbide," *J. Am. Ceram. Soc.*, **72** [1] 49–53 (1989).

[19]T. Ohji and Y. Yamauchi, "Long-Term Tensile Creep Testing for Advanced Ceramics," *J. Am. Ceram. Soc.*, **75** [8] 2304–307 (1992).

[20]T. Ohji, A. Nakahira, T. Hirano, and K. Niihara, "Tensile Creep Behavior of Alumina/Silicon Carbide Nanocomposite," *J. Am. Ceram. Soc.*, **77** [12] 3259–62 (1994).

[21]F. Wakai, S. Sakaguchi, and Y. Matsuno, "Superplasticity of Yttria-Stabilized Tetragonal ZrO_2 Polycrystals," *Adv. Ceram. Mater.*, **1**, 259–63 (1986).

[22]F. Wakai, S. Sakaguchi, Y. Matsuno, and H. Okuda, "Tensile Creep Test of Hot-Pressed Si_3N_4"; pp. 279–85 in *Ceramic Components for Engines: Proceedings of the First International Symposium 1983, Japan.* Edited by S. Sōmiya, E. Kanai, and K. Ando. Elsevier, New York, 1986.

[23]"Elevated Temperature Tensile Creep Strain, Creep Strain Rate, and Creep Time-to-Failure for Advanced Monolithic Ceramics," ASTM Tech. Rept. C1291, American Society for Testing and Materials, Philadelphia, PA, 1995.

[24]T. Ohji, Y. Yamauchi, and S. Kanzaki, "Tensile Creep and Creep Rupture Behavior of HIPed Silicon Nitride"; pp. 569–74 in *Silicon Nitride 93*, Proceedings of the International Conference on Silicon Nitride-Based Ceramics (Stuttgart, Germany, Oct. 4–6, 1993). Edited by M. J. Hoffman, P. F. Becher, and G. Petzow. TransTech Publications, Aedermannsdorf, Switzerland, 1994.

[25]D. R. Wiese and S. Daicos, "Applications for Optical Extensometers," *Adv. Mater. Processes*, **146** [11] 33–34 (1994).

[26]R. H. Marion, "A New Method of High-Temperature Strain Measurement," *Exp. Mech.*, **18** [4] 134–40 (1978).

[27]T. R. Pryor and W. P. T. North, "The Diffractographic Strain Gage," *Exp. Mech.*, **11**, 565–68 (1971).

[28]H. Pih and K. C. Liu, "Laser Diffraction Methods of High-Temperature Strain Measurements," *Exp. Mech.*, **31**, 60–64 (1991).

[29]G. W. Graves, University of Dayton Research Institute, Dayton, OH; personal communication, 1995.

[30]B. W. Christ and S. R. Swanson, "Alignment Problems in the Tensile Test," *J. Test. Eval.*, **4**, 405–17 (1976).

[31]D. R. Hayhurst, "The Effects of Test Variables on Scatter in High-Temperature Tensile Creep-Rupture Data," *Int. J. Mech. Sci.*, **16**, 829–41 (1974).

[32]S. M. Wiederhorn, G. D. Quinn, and R. Krause, "Fracture Mechanism Maps: Their Applicability to Silicon Nitride"; see Ref. 8, pp. 36–61.

[33]W. E. Luecke and S. M. Wiederhorn, National Institute of Standards and Technology, Gaithersburg, MD; unpublished research, 1995. □